



Publication Year	2016
Acceptance in OA	2020-05-27T09:08:59Z
Title	Photo controlled deformable mirrors: materials choice and device modeling
Authors	Quintavalla, Martino, Bonora, Stefano, Natali, Dario, BIANCO, ANDREA
Publisher's version (DOI)	10.1364/OME.6.000620
Handle	http://hdl.handle.net/20.500.12386/25211
Journal	OPTICAL MATERIALS EXPRESS
Volume	6

Photo controlled deformable mirrors: materials choice and device modeling

Martino Quintavalla,^{1,2*} Stefano Bonora,³ Dario Natali¹ and Andrea Bianco²

¹Politecnico di Milano, Piazza L. Da Vinci 32, 20133 Milano, Italy

²INAF, Osservatorio Astronomico di Brera, Via Brera 28, 20121 Milano, Italy

³IFN CNR, Via Trasea 7, 35131 Padova, Italy

*martino.quintavalla@polimi.it

Abstract: Photo Controlled Deformable Mirrors (PCDMs) are electrostatic membrane mirrors where a photoconductive material replaces the conventional electrode pads, so that the mirror surface deforms according to a light pattern projected on the photoconductor, leading to a simplified control system. A proper device design and manufacturing has to take into account many different issues and the material choice is of primary importance. After a brief description of PCDM working principles we consider an equivalent electrical model, deriving the photoconductor's parameters that most influence the device performances and show some examples among currently available photoconductors. Finally, we propose a complete electro-opto-mechanical model that allows to optimize the system and to enhance the mirror performances.

© 2016 Optical Society of America

OCIS codes: (230.0230) Optical devices; (110.1080) Active or adaptive optics; (160.5140) Photoconductive materials; (230.4040) Mirrors.

References and links

1. J. W. Hardy, "Adaptive optics-a progress review," *Proc SPIE* **1542**, 2–17 (1991).
2. F. Roddier, *Adaptive Optics in Astronomy* (Cambridge University Press, 1999).
3. M. J. Booth, "Adaptive Optics in Microscopy," *Opt. Digit. Image Process. Fundam. Appl.* **365**, 2829–2843 (2011).
4. A. Roorda, "Adaptive optics for studying visual function: a comprehensive review," *J. Vis.* **11**(5), 1–21 (2011).
5. B. Sun, P. S. Salter, and M. J. Booth, "Pulse front adaptive optics: a new method for control of ultrashort laser pulses," *Opt. Express* **23**, 19348–19357 (2015).
6. M. Yellin, "Using membrane mirrors in adaptive optics," *Proc SPIE* **75**, 97–102 (1976).
7. R. P. Grosso and M. Yellin, "The membrane mirror as an adaptive optical element," *J. Opt. Soc. Am.* **67**, 399–406 (1976).
8. U. Bortolozzo, S. Bonora, J. P. Huignard, and S. Residori, "Continuous photocontrolled deformable membrane mirror," *Appl. Phys. Lett.* **96** 251108 (2010).
9. N. Sheridan, "The Ruticon family of erasable image recording devices," *IEEE Trans. Electron Devices* **19**, 1003–1010 (1972).
10. S. Bonora, D. Coburn, U. Bortolozzo, C. Dainty, and S. Residori, "High resolution wavefront correction with photocontrolled deformable mirror," *Opt. Express* **20**, 5178–5188 (2012).
11. J. Khoury, A. Drehman, C. L. Woods, B. Haji-Saeed, S. K. Sengupta, W. Goodhue, and J. Kierstead, "Optically driven microelectromechanical-system deformable mirror under high-frequency AC bias," *Opt. Lett.* **31**(6), 808–810 (2006).
12. A. I. Lakatos, "Photoelectric induced elastomer deformation in PVK-TNF type γ -RUTICON," *J. Appl. Phys.* **45**, 4857 (1974).
13. B. Haji-saeed, R. Kolluru, D. Pyburn, R. Leon, S. K. Sengupta, M. Testorf, W. Goodhue, J. Khoury, A. Drehman, C. L. Woods, and J. Kierstead, "Photoconductive optically driven deformable membrane under high-frequency bias: fabrication, characterization, and modeling," *Appl. Opt.* **45**(12), 2615–2622 (2006).

14. M. Cardona and P. Yu, *Fundamentals of Semiconductors - Physics and Materials Properties* (Springer, 2010).
15. D. S. Weiss and M. Abkowitz, "Advances in organic photoconductor technology," *Chem. Rev.* **110**(1), 479–526 (2010).
16. J. Wilson, J. F. B. Hawkes, *Optoelectronics: An Introduction* (Prentice Hall, 1989), 2nd ed.
17. D. Schroöder, *Semiconductor Material and Device Characterization* (John Wiley & Sons, 2006), 3rd ed.
18. I. Ladabaum, X. Jin, H. T. Soh, A. Atalar, and B. T. Khuri-Yakub, "Surface micromachined capacitive ultrasonic transducers," *IEEE Trans. Ultrason. Ferroelectr. Freq. Control* **45**(3), 678–690 (1998).
19. F. Yang, "Membrane modeling of pull-in instability in MEMS sensors and actuators," in *Proceedings of IEEE Sensors* (IEEE 2002), pp. 1199–1203.
20. M. C. Lai, "A note on finite difference discretizations for poisson equation on a disk," *Numer. Methods Partial Differ. Equ.* **17**(3), 199–203 (2001).
21. U. Bortolozzo, S. Residori, A. Petrosyan, J.P. Huignard, "Pattern formation and direct measurement of the spatial resolution in a photorefractive liquid crystal light valve," *Opt. Commun.* **263**(2)317–321 (2006).

1. Introduction

Since Adaptive Optics (AO) has been proposed in the 1950s and implemented about 20 years later as a method to compensate for aberrations in optical systems [1], it led to great progress in many scientific fields such as astronomy, microscopy, ophthalmology, laser pulse shaping and many others [2–5]. In order to perform the wavefront correction, deformable mirrors are widely used. Electrostatic membrane deformable mirrors are used in adaptive optics, in particular, due to some advantages in terms of continuous surface deformation, high actuator density, simple and relatively inexpensive fabrication, curvature proportional to control bias, etc. [6,7]. Among them, Photo Controlled Deformable Mirrors (PCDMs) represent a great simplification in the control system. In these devices, in fact, the conventional electrodes are replaced by a photoconductor and the driving force for the mirror deformation is a light pattern projected on its back side. This configuration takes advantage from well established light modulation technologies, such as liquid crystal displays or digital micromirror devices, allowing for a reduction of the control system complexity since the mirror is directly controlled by the light pattern. Moreover, the absence of heavy/bulky controllers on the back of the mirror makes PCDMs suitable for particular applications where high resolution and light weight or small volume is needed (i.e. telescope secondary mirrors or aerospace applications) [8]. PCDM working principles were already exploited in the '70s to build image recording devices [9], but only recently have proper deformable mirrors been realized and characterized [8, 10, 11].

In the design of a deformable mirror based AO system, the properties of the mirror are usually expressed in terms of aperture size, number of actuators (resolution), maximum stroke and response time (bandwidth). When considering the use of PCDMs however further elements, such as light response and working conditions limits, have to be determined. At the state of the art, some physical models have been proposed to describe them, but, in general, only the maximum membrane displacement as a function of light intensity has been considered [8, 10, 11].

In this paper, after a brief description of the PCDM working principles we consider an electrical model that allows one to understand PCDM's transient and steady state response to light stimuli, highlighting the role of the photoconductor properties and thus allowing for a proper material choice. We then implement a complete electro-opto-mechanical model that describes the mirror behavior and its limits allowing full exploitation of its performance.

2. PCDM working principles

PCDMs are based on a thin reflective membrane which is suspended above a photoconductive substrate as shown in Fig. 1. When a voltage bias is applied between the membrane and the photoconductor, the system gets charged and electrostatic pressure is exerted on the membrane

pulling it towards the photoconductor. As light is shone on a particular area of the photoconductor, charge carriers are generated and dragged by the electric field, increasing the local electrostatic pressure and providing a localized deformation of the membrane.

Depending on the nature of the power supply, the mirror behavior is significantly different: if supplied in DC the deformation is maintained after the illumination unless the electrical bias is removed or thermal generation slowly restores the charge neutrality in the photoconductor. This is due to the fact that once the charge carriers have been generated, the electric field keeps them separated preventing recombination. Conversely, when supplied in AC, charge carriers tend to annihilate at the polarity change of every AC cycle in such a way that when illumination is interrupted the original membrane shape is quickly restored. In this case the membrane is subject to an oscillating attracting force and the position is stabilized by its inertia and surrounding medium (often air) damping. This last operation mode is the most important in AO, since it makes it possible to vary the mirror shape at a very fast rate and it will be discussed in the following sections.

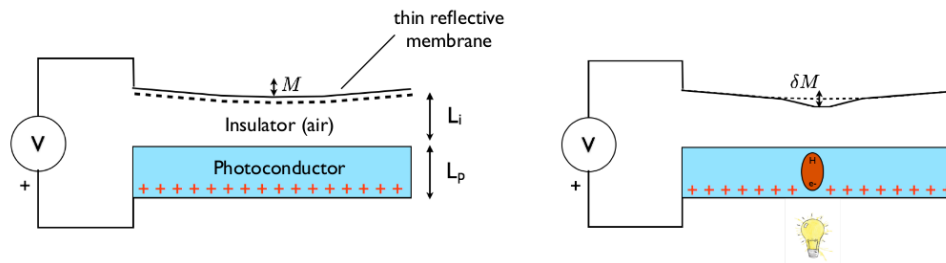


Fig. 1. PCDMs functioning scheme in DC: a) before illumination, b) after illumination.

In both cases the steady state membrane displacement M is related to the electrostatic pressure P_{es} by the Poisson equation

$$\nabla^2 M = -\frac{P_{es}}{T} \quad (1)$$

where T is the membrane tension per unit length and $P_{es} = \epsilon E^2/2$ where $E = V_i/L_i$ is the electrical field and ϵ the dielectric constant of the surrounding medium. In the case of AC power supply V_i is the R.M.S. value of the voltage bias.

3. Electrical modelling

From a purely electrical point of view, PCDMs can be assumed as a double layer dielectric structure and modeled as in Fig. 2. Each layer can be described as a RC system where the resistance in the photoconductive layer is a function of the light intensity. This circuit is a voltage divider and its steady state response has already been described in detail along with the transient DC response [12, 13]. A description of the transient response in AC is however more important for AO applications and will be derived here.

As a first approximation we will consider that the membrane displacement is small with respect to the membrane-photoconductor distance so that the capacitance of the insulating layer will not change after illumination.

Since we want to calculate the membrane displacement, the quantity we need to retrieve is the voltage applied to the membrane V_i .

The current density in the circuit is given by:

$$i = C_p \frac{dV_p}{dt} + V_p G_p = C_i \frac{dV_i}{dt} + V_i G_i \quad (2)$$

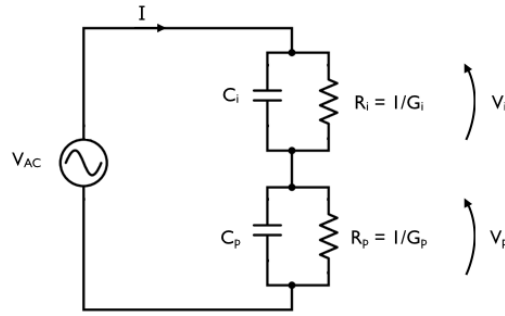


Fig. 2. PCDMs electrical model.

Where $C_x = \epsilon_x/L_x$ and $G_x = \sigma_x/L_x$ are the unit area capacitances and conductances for the insulating ($x = i$) and photoconductive ($x = p$) layer, and L_x is the thickness of the layers.

In order to evaluate the system response to a light step we solved this differential equation considering $V_{AC} = V_0 \exp(i\omega t)$. Neglecting the dark conductance of the photoconductor and the conductance of the insulator, the solution for $V_i(t)$ is:

$$V_i(t) = \left| \left[V_i(0) - \frac{V_0 A}{i\omega + 1/\tau} \right] \exp(-t/\tau) + \frac{V_0 A}{i\omega + 1/\tau} \exp(i\omega t) \right| \quad (3)$$

with

$$V_i(0) = V_{AC} \frac{C_p}{(C_i + C_p)} \quad (4)$$

$$A = (G_p + i\omega C_p)/(C_i + C_p) \quad (5)$$

This solution is valid assuming that the conductances are independent on the electric field which is a valid approximation for most inorganic photoconductors [14].

The characteristic response time of the system is:

$$\tau = \frac{\epsilon_i + \epsilon_p(L_i/L_p)}{\sigma_p(L_i/L_p)} \quad (6)$$

τ depends on the material's dielectric constant and conductivity, as well as on the geometrical characteristics of the PCDMs in terms of ratio of the layers thicknesses.

Another important quantity that can be derived is the dynamic range, expressed as the ratio $|V_i^{RMS}(light)|/|V_i^{RMS}(dark)|$ that describes how much the electric tension V_i varies from dark to light:

$$\left| \frac{V_i^{RMS}(light)}{V_i^{RMS}(dark)} \right| = \left| \frac{\sigma_p/\epsilon_p + i\omega}{\frac{\sigma_p(L_i/L_p)}{\epsilon_e + \epsilon_p(L_i/L_p)} + i\omega} \right| \quad (7)$$

Such ratio also depends on the same material's properties and on the ratio L_i/L_p .

From these results it is evident that, in order to have a fast response and a wide dynamic range of the PCDM, a suitable photoconductor should have a low dielectric constant and a high conductance when illuminated. The ratio L_i/L_p plays a more complicated role. As it decreases (thick photoconductor), the dynamic range is improved, however the response time of the system is slowed down. A proper design has to take this trade-off into account when choosing a photoconductor with a specific thickness.

In the following section the role and the importance of the various properties will be highlighted with simulations.

4. Photoconductors for PCDMs

According to the previous description, finding a suitable photoconductor among all the different classes of materials is a complex task. PCDMs reported in literature are based on inorganic crystals such as bismuth silicon oxide (BSO) and GaAs that are characterized by a high dielectric constant (typically greater than 10) whose limiting effect is compensated by the high mobility, as in the case of GaAs, or high thickness as for BSO. Among other classes of materials, organic photoconductors (OPC) are promising due to their low dielectric constant (~ 4), easy processability from solution and scalability. Their advantages are however limited by the low mobility, significant dark conductance and low thickness [15]. Values of dielectric constant and mobilities for these materials are reported in table 1.

In the following we will make a comparison among some selected materials, in order to understand the capabilities of each one in terms of response time and dynamic range. For this purpose we will consider a simple photoconduction model that correlates conductance to light intensity assuming that photon energy is high enough to promote the transition of electrons from the valence to the conduction band (i.e. if the wavelength is below the absorption threshold) [16]. In photoconductors with a negligible dark charge carrier density (undoped and with a high energy gap), the conductance due to illumination with monochromatic light can be expressed as:

$$\sigma_{light} = \frac{\eta \tau_c I (\mu_e + \mu_h) e}{h\nu L_p} \quad (8)$$

Where $h\nu$ is the photon energy, η the quantum efficiency (number of carriers generated per absorbed photon), τ_c the mean carrier lifetime, μ_x the mobilities for electrons and holes, e the electron charge and I the absorbed light intensity.

Following this approach we have run simulations considering the following materials: BSO, GaAs, ZnSe and organic photoconductors (OPCs). The first two are reference materials used in previous works, ZnSe is an example of commercially available thick photoconductor that can be used with visible light, while OPCs are a class of materials still under development that are very promising for this application.

In order to compare them we will consider a typical photoconductor-membrane distance of $50 \mu\text{m}$ as reported in [10] and 10^{-7} s as reasonable values for the product $\eta \tau_c$ for every material. The values for dielectric constant, mobilities, illumination wavelength corresponding to the energy gap and typical thickness of these materials are reported in table 1. Using these

Table 1. Physical characteristics of some selected photoconductors reported from [15, 17].

Photoconductor	ϵ_R	μ_e	μ_h	λ_{Eg}	Thickness (typ.)
	-	cm^2/Vs	cm^2/Vs	nm	mm
BSO	55	3.5	$\sim 10^{-2}$	390	3
GaAs	12.8	8500	400	870	1
ZnSe	9.25	540	30	460	3
OPCs	~ 4	$\sim 10^{-8}$	$\sim 10^{-6}$	$400 \div 800$	3×10^{-2}

values, along with equations (6), (7) and (8) we can calculate the PCDM performances as a function of the illumination intensity under the hypothesis of negligible dark conductance and

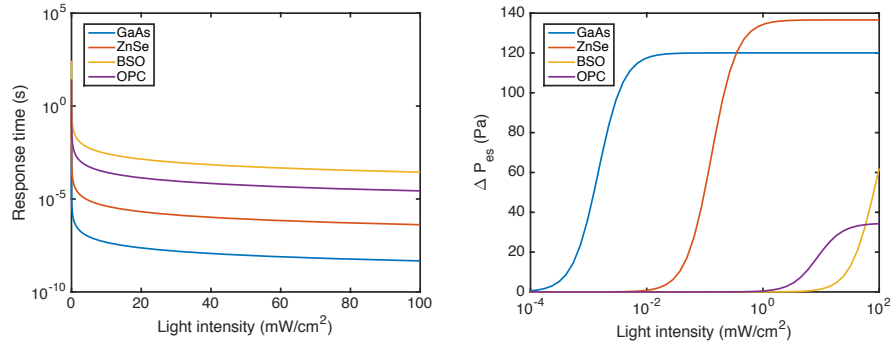


Fig. 3. Electric simulation of PCDM performances as a function of the illumination intensity with different photoconductors. Left: response time, right: dynamic range.

homogeneous charge generation along the photoconductor thickness. A simulation for working conditions of 400 Vpp at 500 Hz is reported in Fig. 3 where the response time and the dynamic range expressed in terms of electrostatic pressure variation are reported as a function of the light intensity.

It is clear that response time and dynamic range can be very different depending on the considered materials. In particular, materials with higher mobilities show a very short response time and their response to light in terms of dynamic range saturates for very low light intensities restricting the dynamic control to a very narrow region. The maximum achievable dynamic range instead, depends mainly on the ratio L_p/ϵ_p rather than on the other parameters. In the case of organic photoconductors the very low thickness compensates for the low mobility giving a short response time but limiting the dynamic range. It is also noticeable that, since conductivity depends on the charge carrier density, it is inversely proportional to the photoconductor thickness as reported in expression (8). As a consequence, a high thickness means a wider dynamic range but would require more light to exploit it.

5. A comprehensive finite-differences PCDM model

The previous electrical model provides a quite accurate description of PCDMs, especially for small membrane displacements, and important guidelines for the choice and optimization of the photoconductor. However, when it is desired to determine the mirror response for large displacements and deploy all the possible dynamic range, some physical limitations must be considered.

If the local deformation of the membrane exceeds a certain limit, the pulling force due to electrostatic pressure overwhelms the restoring elastic force and the membrane snaps-through to the photoconductor, this is the so called "pull-in instability" effect. This phenomenon has already been studied in the literature for electrostatic membrane devices [18,19]. In these cases, a deformation limit of about one third of the electrode-membrane distance was calculated. Moreover, as the membrane gets closer to the pull-in instability threshold, its behavior becomes different from that predicted with approximated low-displacement models, making the control less accurate.

Another issue to be considered regards the exceedance of the dielectric breakdown threshold by the local electrical field V_i/L_i . In this case electric discharge can lead to control failure and PCDM damage.

In previous works about PCDMs or similar membrane-based optical devices, the determination of the membrane displacement by solving the Poisson equation (see Eq (1))

was always carried out either considering first-order approximation solutions, valid only in case of uniform illumination [6,8,13], or by numerical methods such as finite-differences, often considering the membrane displacement as negligible when computing the capacitance C_i that is considered fixed. Both these methods however can calculate the membrane shape only for small displacements.

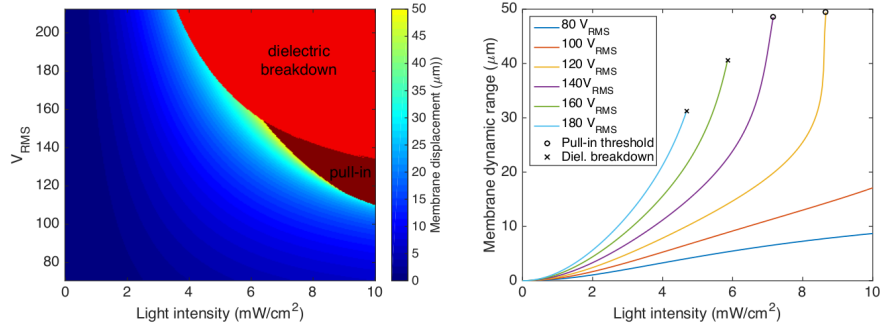


Fig. 4. 1” diameter ZnSe based PCDM finite-differences simulation. Left: dynamic range as a function of the applied voltage and light intensity at 100 Hz in conditions of uniform illumination. ZnSe thickness 3 mm, membrane-photoconductor distance 50 μm , membrane tension 50 N/m. The dynamic range is calculated as $M_{light} - M_{dark}$ at the centre of the membrane. Right: section view at various applied voltages. The zones of dielectric breakdown threshold and membrane pull-in are highlighted.

In order to take the described effects into account, Eq. (1) has to be solved considering that the electrostatic pressure P_{es} at every point is a function of the membrane displacement M .

$$\nabla^2 M(\rho, \theta) = -\frac{P_{es}(M(\rho, \theta))}{T} \quad (9)$$

Due to the intrinsic difficulties in solving the equation analytically, it is advantageous to solve it by means of some numerical method. In particular, having often PCDMs of a circular shape, we adopted a finite differences solution for the Poisson equation on a circular domain in cylindrical coordinates [20]. In order to consider nonlinearities and evaluate dielectric breakdown and pull-in instability threshold, the equation has been solved iteratively, starting from the initial condition of flat membrane ($M = 0$). The local electric field is evaluated at each iteration, adopting the electrical model described above and considering that the new membrane position affects the local distance L_i and so the local capacitance.

For sake of simplicity, in this calculation, the transversal charge diffusion in the photoconductor due to coulombic repulsion and thermal effects has not been considered. A more complex electrical modeling would be required to consider it and obtain a more realistic simulation. In general, however, for crystalline photoconductors this effect is small (of the order of tenths of microns) [21]. The iteration is terminated if the membrane position converges within a given tolerance (10 nm) or is interrupted if the membrane position diverges, meaning that the pull-in instability threshold has been reached, or the electric field $E_i = V_i/L_i$ in the gap between the membrane and the photoconductor exceeds the breakdown threshold.

By means of this analysis it is possible to determine the PCDM safe working conditions in terms of power supply voltage, frequency and light intensity and to identify the working zone allowing to exploit the maximum dynamic range ($M_{light} - M_{dark}$) or the most convenient one in terms of light response and linearity. Regarding the dynamic range, we have to point out that it is limited by the spatial response of the membrane. As a general statement, increasing the

spatial resolution of the light actuators, a smaller dynamic range can be achieved, due to the membrane low-pass filter behavior.

An example of the results obtained with this method for a 1" zinc selenide based PCDM is shown in Fig. 4.

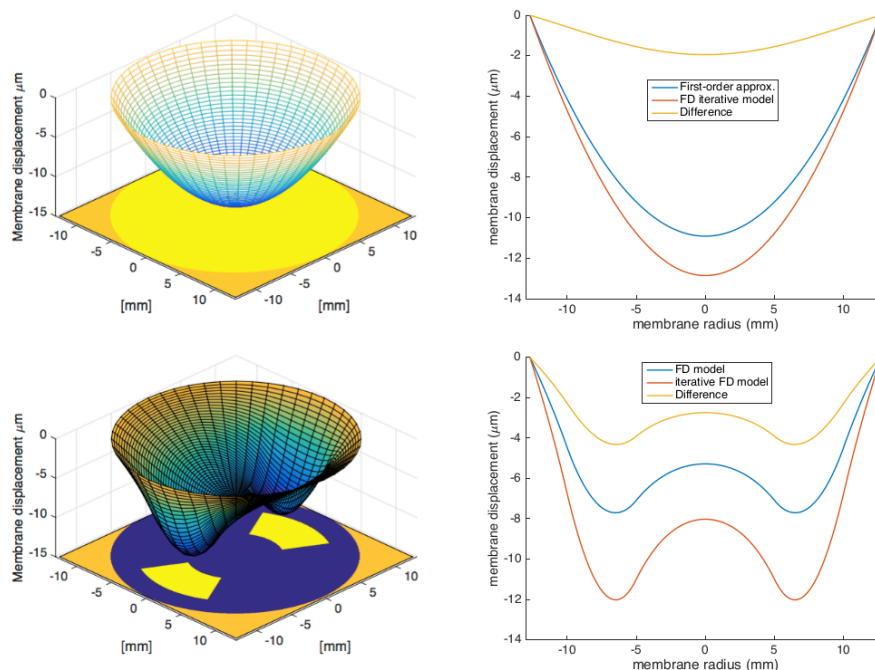


Fig. 5. Examples of a 1" diameter ZnSe-based PCDM response to the light patterns depicted at the bottom of the plots on the left. Blue zones: no light, yellow zones: 10 mW/cm², orange zones: outside the PCDM region. The comparison between approximated model of [8, 13], finite difference (FD) model and our iterative FD model is shown in the sections on the right. Simulations were run with the following parameters: 200 V_{PP}, 100 Hz, ZnSe thickness 3 mm, membrane-photoconductor distance 50 μm, membrane tension 50 N/m.

From these simulations it is evident that the driving voltage has a noticeable influence on the device's behavior: a lower voltage leads to a more linear correlation between light intensity and membrane displacement, while a higher voltage, despite increasing the dynamic range, tends to make the mirror more sensitive to light and hence the control of the deformation is not reliable, especially approaching the pull-in threshold or the dielectric breakdown limit.

Regarding the pull-in instability threshold, we noticed that in some conditions it is close to the physical photoconductor-membrane distance, therefore much larger than the predicted values for electrostatic devices ($\sim 0.38L_i$ [19]). Such a discrepancy is due to the presence of the photoconductor. Considering the scheme of Fig. 2, in fact, when the distance L_i is reduced, the capacitance of the membrane increases hence its impedance decreases and most of the voltage bias drops across the photoconductor. For this reason the pull-in threshold can be higher than that of normal electrostatic devices.

With this approach it is also possible to determine the shape assumed by the membrane as a consequence of the illumination with an arbitrary light pattern, with a higher accuracy with respect to ordinary finite-difference methods. To show the capability of this method, two significant examples have been analyzed: a case of uniform illumination and a particular light

pattern constituted by two opposite lit zones. The outcome of the analyses has been compared with the one obtained with the simplified low-displacement models [8, 13] in the case of uniform illumination and with ordinary finite-differences in the other and the results are reported in Fig. 5.

From the results obtained, it is interesting to note that the membrane position differs significantly from the one predicted by ordinary models, underlining the need for a comprehensive model when dealing with consistent membrane deformations. In the case of an arbitrary light pattern, simulations (reported in Fig. 5) show that it is possible to determine accurately the membrane shape, demonstrating that this method constitutes a very powerful tool to predict the optical response of a PCDM-based AO system.

6. Conclusion

In this paper the behavior of Photo Controlled Deformable Mirrors has been analyzed, highlighting the role of the photoconductor properties. In particular, the working principle of PCDMs both in DC and AC regime has been illustrated and from an electric modeling it has been possible to understand which properties influence the device's performance in terms of response time and dynamic range. Simulations based on the electric model have been applied to selected photoconductors in order to demonstrate how the materials choice can influence the device's performance. This allowed one to understand that, considering reasonable geometries, charge carrier mobility mostly influences the response time, while thickness and relative dielectric constant influence the dynamic range. Finally a finite-differences based electro-optomechanical model has been implemented in order to consider further practical aspects that can limit the operation of the device such as pull-in threshold and dielectric breakdown threshold, allowing for the first time to identify the safe working zone in terms of voltage bias, light intensity and frequency and to determine the most convenient working conditions in terms of light response and linearity. Two examples have been shown, highlighting that a much higher predictability can be achieved with respect to other literature models.